

Flow and magnetic field induced collagen alignment

Cheng Guo, Laura J. Kaufman*

Department of Chemistry, Columbia University, New York, NY 10027, USA

Received 9 August 2006; accepted 9 October 2006

Available online 16 November 2006

Abstract

A straightforward technique to align thin collagen gels is presented. This technique requires only collagen solution, surface-modified magnetic beads, a small magnet, and an incubator. As such, this is the only collagen alignment technique that requires no specialized equipment. The collagen gels are imaged with confocal reflectance microscopy, and degree of alignment is quantitatively assessed using image analysis techniques that allow for identification of fiber position and angular distribution. A series of experiments shows that magnetic beads coated with streptavidin lead to the most highly aligned gels. Rheology and microscopy experiments suggest that alignment results from bead coupling to, and entrainment and entrapment in, collagen fibrils during their assembly into fibers that form a sample-spanning gel. The timescales of gelation and bead motion to the poles of the external magnet must be similar to effect good alignment over large areas with this technique. It is also demonstrated that alignment can be attained in both plain and cell-bearing gels that are several millimeters thick.

© 2006 Elsevier Ltd. All rights reserved.

Keywords: Collagen; Confocal microscopy; Material properties; Self assembly

1. Introduction

Collagens are proteins composed of three polypeptide subunits known as α -chains that exist in a unique triple-helix. More than 20 types of collagen, which vary in the length of helix and nature and size of the non-helical portions, exist in animal tissue [1]. Many of these collagens self assemble into large-scale structures under physiological conditions. These large-scale structures offer high-tensile strength and exist in a wide variety of tissue-specific geometries that provide a stable architecture for those tissues [2,3]. Indeed, collagen is the most prevalent structural protein in the complex microenvironment, known as extracellular matrix (ECM), that surrounds and supports animal cells.

Type I collagen is the predominant form of collagen in animal tissue and is found in large quantities in skin, tendon, and bone. The collagen I molecule is composed of two identical $\alpha 1(I)$ chains and one $\alpha 2(I)$ chain. The rod-like

triple-helical protein is 1.5 nm in diameter and 300 nm in length and undergoes self-assembly into macromolecular fibrils with a width of 36 nm, which in turn associate to form fibers and fiber bundles [1,4–7]. The initial assembly into fibrils is both thermodynamically spontaneous and endothermic, though it has been debated whether this process is driven by the increase in entropy associated with loss of water from the bound monomers [5] or by hydrophilic interactions [8]. In vivo, as collagen I fibrils organize into fibers and grow in width and length, they can organize into extensive parallel arrays, as in tendons and ligaments, or into regular sheets in which fiber orientation changes abruptly from layer to layer, as in the transparent cornea of the eye [9,10]. More typically, collagen I fibers become arranged randomly, constituting an isotropic structural network in the so-called irregular connective tissues.

Isotropic collagen I matrices have long been used as an approximation to ECM on (two-dimensional (2D) substrates) or in (three-dimensional (3D) matrices) which to study cell behavior. These isotropic systems are straightforward to prepare in vitro [11–13]. Because the fibers

*Corresponding author. Tel.: +1 212 854 9025; fax: +1 212 932 1289.

E-mail address: kauffman@chem.columbia.edu (L.J. Kaufman).

produced from collagen I molecules under physiological conditions are typically several hundred nanometers in diameter and tens of microns in length [1,11,14], they give rise to substantial Mie scattering. As a result, collagen fibers comprising such a matrix are easily imaged by confocal reflectance microscopy (CRM) [15,16], a non-perturbative microscopy with 3D resolution. Imaging cells embedded in such collagen matrices simultaneously with the collagen itself has allowed detailed study of physiological processes in which cell migration and matrix remodeling are important, such as wound healing and cancer cell invasion [13,17–26].

While it is straightforward to prepare isotropic 2D and 3D arrays of collagen (though it should be noted that at least one study found such systems not to be truly isotropic [27]), assembling aligned 2D and 3D collagen systems is more challenging. Such systems are desirable for a variety of reasons. First, to mimic processes that occur in dense regular connective tissue like tendons and ligaments, aligned collagen is necessary. Second, to tease out the importance of mechanical properties on cell behavior, it is useful to challenge cells with a variety of surroundings including anisotropic ones such as those provided by aligned collagen gels. Finally, the ability to produce aligned sheets of collagen fibers allows for construction of scaffolds that mimic the alternating sheets of collagen fibers found in bone and corneal tissue [10,28].

The earliest reported *in vitro* aligned collagen systems were formed using an electrical gradient by Benjamin et al. [29]. The first widely recognized *in vitro* collagen alignment was performed by Elsdale and Bard [30] via a drainage technique, which involves gravity-driven flow. This technique was extended by Mosser et al. [31] to prepare very high-concentration collagen matrices that display a variety of liquid crystalline types of order. Several other groups have developed ways to align collagen fibers that lead to more regular alignment over larger areas. The most common of these techniques involves exposing collagen solution to a strong static magnetic field on the order of 1 T during gelation [17–19,21,32]. Here, the fibrils form perpendicular to the field, as each collagen molecule has a small negative diamagnetic susceptibility [33,34]. The regular organization of such molecules into fibers leads to a large enough negative diamagnetic susceptibility along the fibers to effect such alignment [32]. More recently it has been shown that applying interstitial fluid flow to collagen gels disentangles fibers in a previously entangled, isotropic network and results in an aligned gel perpendicular to the flow field [35,36]. Also, flow of a collagen solution through a microfluidic channel up to $\sim 100\ \mu\text{m}$ in width during gelation results in collagen fibers aligned along the direction of flow [37]. However, an easy and effective way to make highly oriented collagen gels with no specialized equipment has not yet been demonstrated. In this work, we describe a technique that allows preparation of thin gels of aligned collagen using magnetic beads and a small magnet.

2. Experimental

2.1. Materials

Purified, pepsin-solubilized bovine dermal type I collagen (Vitrogen 100, FXP-019) is mixed with phosphate buffered saline (PBS) (Sigma, $10\times$) and NaOH (0.1 N) to prepare a collagen solution with pH between 7.2 and 7.4 and concentration of 2.5 mg/ml. Six types of paramagnetic iron oxide beads have been employed: streptavidin coated (Bangs Labs, BM551), primary amine modified (Bangs Labs, BM546 and Kisker, PM-2.5), carboxyl modified (Bangs Labs, BM570 and Kisker, PMC-2.5), and unmodified (Kisker, PMN-2.5) iron oxide beads. Particles from Bangs Labs are not strictly spherical but have average diameter of $1.5\ \mu\text{m}$. All beads from Bangs Labs are silanized iron oxide, and are $>90\%$ iron oxide by weight. No iron oxide is exposed on the bead surface. The particles from Kisker are spherical, have an average diameter of $2.5\ \mu\text{m}$ and consist of a polystyrene (PS) core coated with iron oxide and another layer of PS. Again, no iron oxide is exposed.

2.2. Thin gel preparation

Preparation of the collagen solution and mixing with the magnetic beads is done rapidly at $\sim 4^\circ\text{C}$ to limit self-assembly of the collagen molecules before loading into the sample cell and placement in an incubator. The beads are added to the 2.5 mg/ml collagen solution at concentrations between 0.01 and 0.1 mg/ml. For preparation of the thin gels, $10\ \mu\text{l}$ of the collagen or collagen/bead solution is pipetted onto a microscope slide and covered with a coverslip. The edges are sealed with epoxy, taking care not to allow any epoxy to seep into the sample. These samples have thickness of $10\text{--}20\ \mu\text{m}$. A magnetic stir bar (VWR, 58948-397) with field strength $<1\ \text{G}$ at the poles as measured by a Gaussmeter is placed either atop the coverslip or underneath the glass slide. The field lines produced by the oblong magnetic stir bar are as expected for a dipolar oblong object. This was confirmed by an experiment in which iron filings were placed in a sample cell with the magnetic stir bar atop the sample cell. Though all thin gel data discussed in this manuscript are achieved with placement of the magnet atop the coverslip, similar alignment results from placement underneath the glass slide. Ten thin gels prepared with each of the six types of magnetic beads (streptavidin-coated beads, large amine modified beads, small amine modified beads, large carboxyl modified beads, small carboxyl modified beads, and unmodified beads) are prepared for image analysis.

2.3. Thick gel (and embedded cell) preparation

Though the focus of this manuscript is on the degree and mechanism of alignment in thin gels, similar results can be obtained in thicker gels. Here, cylindrical sample cells (1 cm diameter plexiglass cylinders of 1 cm height with a glass coverslip forming the bottom of the sample cell) are employed. In cell free samples, 2.5 mg/ml collagen and 0.1 mg/ml magnetic bead solution is prepared. Here, a stronger ($\sim 2\ \text{G}$), cylindrical magnet (McMaster, 5862K32) is placed adjacent to the sample cell during fibrillogenesis, rather than atop it. Thick aligned gels can also be prepared with cells embedded in the matrix. In this case, collagen solution is prepared with a recipe used previously [13] containing collagen, PBS, $1\times$ DMEM, fetal bovine serum, antibiotics, and NaOH. This collagen solution, magnetic beads, and cells (C6 glioma) at $\sim 1\times 10^6$ cells/ml are added to the sample cell. The final collagen concentration in these samples is 1.2 mg/ml, and the final magnetic bead concentration is 0.1 mg/ml. Again, a magnet is placed adjacent to the sample cell in an incubator for fibrillogenesis. The plain and cell-bearing gels produced in this manner are several millimeters thick. Though the collagen concentration varies between the plain and cell-bearing thick gels, similar alignment is found in both types of gels. Indeed, alignment of the thick gels appears less sensitive to small variations in conditions than does that of the thin gels.

2.4. Fibrillogenesis

To achieve both self-assembly of the collagen molecules into fibers and alignment of the matrix (as well as to ensure cell health in the gels with embedded cells), the samples and the external magnet are placed in an incubator (37 °C) for at least 30 min. Fibrillogenesis is usually done in an external incubator at 37 °C and 5% CO₂. In situ fibrillogenesis is also performed since it allows imaging during aligned gelation. Here, a homebuilt objective heater and a microscope incubator (Neue Biosciences) at 37 °C and 5% CO₂ are employed.

2.5. Rheology

The time dependent viscous and elastic moduli of collagen samples during gelation are measured using a constant stress rheometer (TA AR-2000). A 1° acrylic cone geometry with a solvent trap is used, and experiments are conducted in the oscillatory mode. The rheometer is equipped with a temperature control unit that allows heating the sample to 37 °C. The time-dependent elastic and viscous moduli of the gelling samples are measured at frequencies between 0.1 and 1 Hz with a maximum strain of 0.08.

2.6. Microscopy

An inverted confocal laser scanning microscope (Olympus Fluoview 3000) with a 60 ×, NA = 1.42 oil objective (Olympus PlanApo) or a 20 ×, NA = 0.75 air objective (Olympus Plan S-Apo) and a 633 nm Helium Neon laser are employed to obtain CRM images of the collagen fibers. Supplementary images have been collected with differential interference contrast (DIC) microscopy using the 20 × objective.

3. Results and discussion

3.1. CRM image analysis

To determine alignment (reported in Table 1), 10 thin gel samples of each type are prepared, and visual inspection is used to determine whether there is excellent, good, or no alignment in these samples. An example of a matrix with excellent alignment is shown in Fig. 1c. Such matrices are clearly aligned, and few fibers lay in directions other than that of the overall alignment. An example of a matrix with good alignment is shown in Fig. 1d. Such matrices have an identifiable overall alignment in a particular direction, but

the alignment is less uniform and there is a larger distribution of fiber angles. Examples of matrices with no alignment are shown in Figs. 1a and b. These matrices appear isotropic by visual inspection.

Three typical samples of each type represented in Table 1 are chosen for further processing to quantify collagen alignment. Starting at the upper left hand corner of the image, small sets of pixels (~10) are evaluated for brightness. Once a pixel set with brightness above a certain threshold value is identified, all neighboring pixel sets are searched for similar brightness. If such pixel sets are identified, steps continue within a certain angular distribution around the line defined by the center of the first two pixel sets. This procedure allows accurate identification of fibers even in the presence of fiber entanglement. When there are no longer any bright pixel arrays in the searched area, the fiber is assumed to end. The angle of the fiber relative to a column, defined as 0°, is determined. Then, the pixels making up that fiber are set to have zero intensity before the search procedure continues. This assures no overcounting of fibers. Fibers within the 18 representative images are identified, and the angular distribution of fibers is plotted and fit to a Gaussian for each image (Fig. 2). This quantitative image analysis confirms that there are differences between excellent, good, and unaligned matrices as categorized by visual inspection. In matrices identified visually as displaying excellent alignment, the angular distribution of fibers is well fit by a Gaussian with a full-width half-maximum (FWHM) of less than 40°. In matrices identified as displaying good alignment, the angular distribution of fibers is well fit by a Gaussian, typically with FWHM of 55–75°. In matrices identified as having no alignment, the angular distribution of fibers cannot be well fit by a Gaussian.

3.2. Degree of alignment in thin gels

Collagen solutions prepared without magnetic beads and placed in an incubator for fibrillogenesis without an external magnet form isotropic gels (Fig. 1a). Collagen

Table 1
Collagen alignment effected by magnetic beads

Bead surface modification	Bead diameter (μm)	Number of trials (of 10) exhibiting excellent alignment	Number of trials (of 10) exhibiting good alignment	Average FWHM of Gaussian fit to angular distribution histogram (degrees)
Streptavidin	1.5	3	5	38.5
Amine	1.5	1	6	65.2
Amine	2.5	0	6	72.0
Carboxyl	1.5	0	5	53.8
Carboxyl	2.5	1	4	71.0
None	2.5	0	2	127.2*

All 1.5 μm beads are aspherical and >90% iron oxide. All 2.5 μm beads are spherical and have a polystyrene core. Bead concentration is 0.06 mg/ml in all cases. Excellent versus good alignment is determined as described in the text. Degree of alignment is ascertained by identifying fibers near a pole of the external magnet in three samples prepared in the same manner, constructing a histogram such as that in Fig. 2b for each sample, fitting to a Gaussian, and reporting the average FWHM of the Gaussian for each type of bead. The asterisk on the FWHM reported for the unmodified beads indicates that only one of the three analyzed samples was well fit by a Gaussian, and the FWHM for this sample is reported.

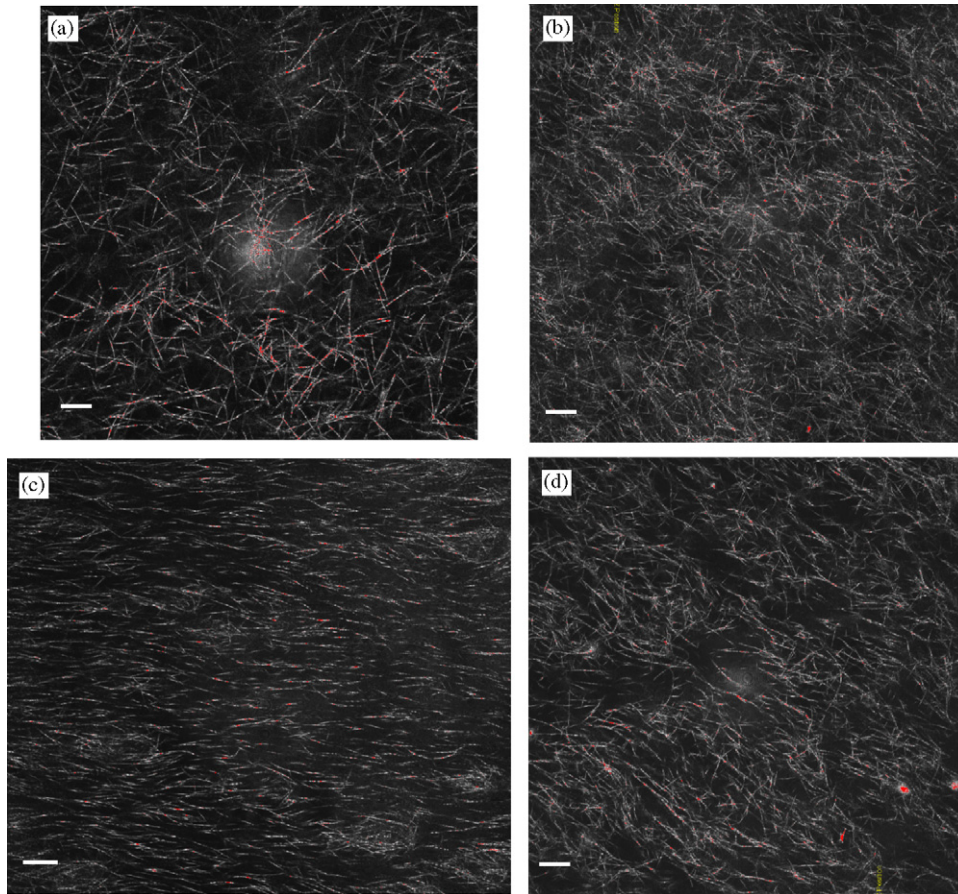


Fig. 1. (a) Collagen (2.5 mg/ml in all figures) incubated with neither magnetic beads nor an external magnet. (b) Collagen incubated with unmodified-magnetic beads and an external magnet. (c) Collagen incubated with streptavidin-coated magnetic beads and an external magnet. (d) Collagen incubated with 2.5 μm amine surface-modified magnetic beads and an external magnet. Scale bar is 15 μm in all images.

solutions with no magnetic beads but with an external magnet placed atop the coverslip during gelation lead to isotropic gels, as do collagen solutions with magnetic beads that are gelled in the absence of an external magnet. Collagen solutions prepared as described in the experimental section with unmodified iron oxide beads and an external magnet present during gelation also typically form isotropic gels (Fig. 1b). In contrast, collagen solutions prepared with streptavidin, amine, and carboxyl modified iron oxide beads in the presence of an external magnet form aligned gels (for example, Figs. 1c and d). In some aligned matrices, few or no clusters of magnetic beads are visible and in some (see, for example, Fig. 3 and Supplementary Movie 1 [38]) more clusters are apparent. All gels are 10–20 μm thick, and the aligned gels contain between 13 and 25 layers of aligned collagen fibers. For external magnet placement atop the coverslip, alignment is best from several microns above the coverslip to the glass slide. After gelation, most of the magnetic colloids are located in elongated clusters along the field lines at the coverslip. The degree of alignment in the x - y plane varies as a function of position relative to the external magnet with the best alignment in an area of several square millimeters near the poles of the magnet. Fig. 3 shows

CRM and DIC images of a thin gel with regions of excellent alignment over a larger area than is displayed in Figs. 1 and 2. Degree of alignment also varies with magnetic bead concentration and surface modification (Table 1). Indeed, a series of experiments has shown that for a collagen concentration of 2.5 mg/ml, alignment can be attained for a variety of magnetic bead types at concentrations between 0.05 and 0.10 mg/ml. Degree of alignment is ascertained as described in Section 3.1. Excellent alignment is only found consistently when employing streptavidin-coated magnetic beads. Good alignment is found consistently when using iron oxide beads coated with streptavidin or modified with carboxyl or amine groups. Excellent alignment has never been achieved and good alignment is rare when employing plain iron oxide beads of the same size and preparation as the other beads employed.

The alignment that we attain in the thin gels can be compared to that which others have attained in thick gels using other alignment techniques. While the techniques employed here for image analysis differ from those employed by Ng et al. [36], the images can be directly compared since both are recorded with CRM. Both alignment methods generate similarly highly aligned gels as assessed by visual inspection. It is more difficult to

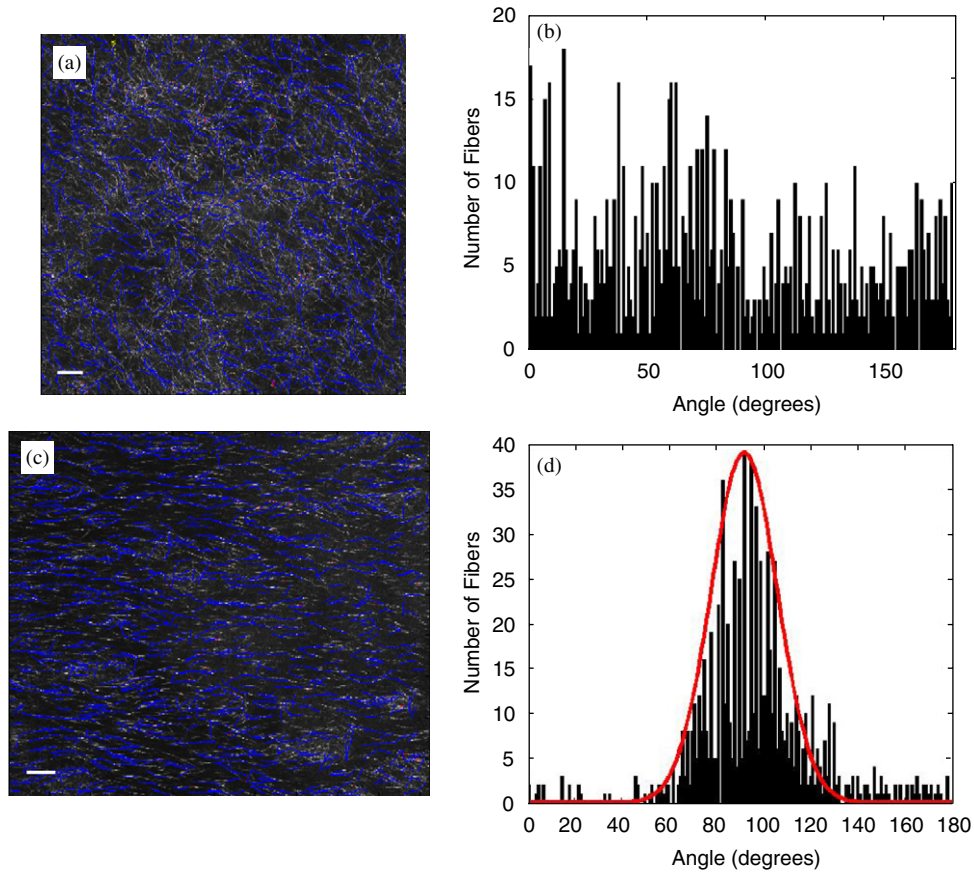


Fig. 2. [Color online.] (a) Fig. 1b overlaid with fibers identified by a program written for this purpose (blue). (b) Histogram of the angular distribution of fibers in Fig. 2a. (c) Image of aligned collagen fibers shown in Fig. 1c overlaid with identified fibers (blue). (d) Histogram of the angular distribution of fibers in Fig. 2b. Scale bar is $15\mu\text{m}$ in both images.

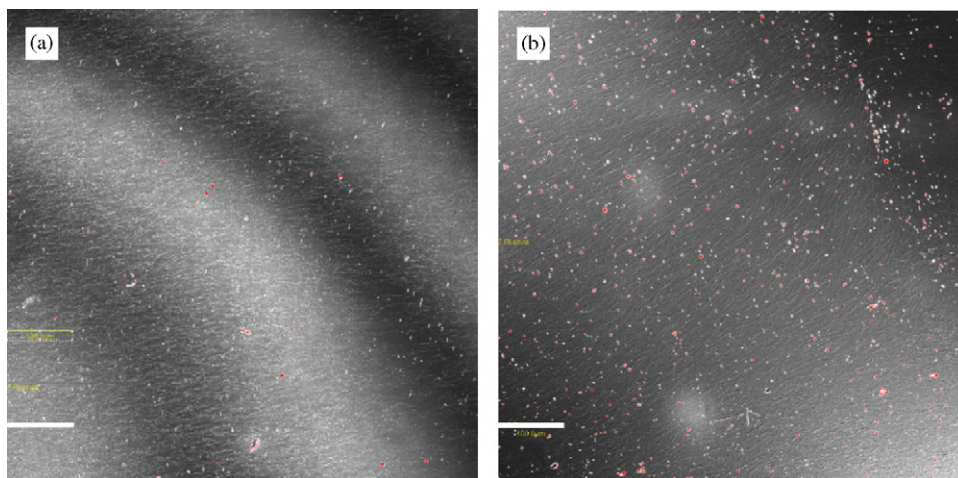


Fig. 3. (a) Low-magnification CRM image of a well-aligned thin gel. Striations are due to Airy rings as well as constructive and destructive interference from reflections from glass above and below the thin gel. (b) Low-magnification DIC image of a well-aligned thin gel. Both images are collected with a $20\times$ objective. Scale bar is $100\mu\text{m}$ in both images.

compare the degree of alignment in our gels to those attained using high-magnetic fields, since those systems have generally been investigated with low-magnification polarized light microscopy and quantified via careful

measurement of birefringence induced by the aligned matrices. However, comparison of our CRM images in Figs. 1 and 2 to the high-magnification image in Ref. [17] shows that we attain qualitatively better alignment on short

length scales [17]. Further, comparison of low-magnification polarized light images in Ref. [17] to the low-magnification images shown in Fig. 3 demonstrates that over longer length scales our thin gel systems appear to be at least as well aligned as those thick gel systems.

3.3. Possible mechanism of thin gel alignment

Aligned collagen gels have previously been formed through mechanisms related to both flow [30,31,35–37] and magnetic field [17–19,21,22,32]. The alignment achieved through the technique we present here, however, is caused by neither flow nor field alone. First, because no alignment is found in systems without magnetic beads but with an external magnet, it is clear that the alignment is not due to the interaction between the external magnet and the inherent diamagnetic susceptibility of collagen fibrils. This is expected, as the field produced by the external magnet used here (less than 1×10^{-4} T) should not be sufficient to orient a collagen fibril that is expected to have between 10^4 and 10^6 collagen molecules, each with a diamagnetic susceptibility on the order of -1×10^{-25} JT⁻² [32]. Further, if the field from the external magnet alone was driving alignment, collagen fibers would be expected to align perpendicular to the field lines; however, they align along the field lines. Another possibility is that in the presence of the external magnet, the paramagnetic beads generate a field that together with that of the external magnet is strong enough to align individual collagen fibers. We discount this mechanism for two reasons: first, it is not expected that fields produced in this manner would be strong enough to effect alignment; second, the magnetic particles are not homogeneously distributed in the gel, and excellent alignment often exists in areas with few beads, where the induced fields would be very small. Further, unless the beads were distributed in a biased way by the external magnet, such a mechanism would not lead to large-scale alignment in any particular direction. So, the alignment is not solely attributable to magnetic field effects. Our results also demonstrate that the alignment can not solely be attributed to flow fields set up as the magnetic beads move along the field lines to the poles of the external magnet as gelation occurs. If this were the case, alignment would result not only when employing streptavidin, carboxyl, or amine modified iron oxide beads but also when employing unmodified iron oxide beads. While the alignment in our system can not be attributed solely to magnetic field effects or flow for the reasons described above, both effects appear necessary to produce aligned collagen in the technique described here. We believe the alignment results from flow created by beads entrained or enmeshed in collagen fibrils as they move towards the magnetic poles, and that the alignment of collagen gels presented here depends on the presence of magnetic beads that adhere to collagen fibrils *during* gelation. The entrapment of the beads is evidenced by the fact that even before gelation is complete the beads become fixed and do

not move when the external magnet is removed and when subjected to both gravity and the field of a stronger external magnet. It is also clear that the timescales of gelation and bead arrival at the magnet must be comparable for alignment to occur. The importance of the relative timescales for gelation and magnetic bead arrival at the magnet is evidenced by the fact that similar experiments carried out with external magnets both weaker and stronger than the one described here do not result in well-aligned matrices.

Collagen matrices (without magnetic beads) at the concentration, pH, ionic strength, and gelation temperature described here are found to gel in approximately 18 min as measured by bulk rheology at 0.5 and 1.0 Hz (Fig. 4a). The final moduli measured are consistent with those measured previously [39]. The dynamics of gelation measured here are difficult to compare to previous rheological studies since those studies were performed at much lower temperatures [12], and collagen gelation kinetics have been shown to be strongly temperature dependent [40,41]. In bulk rheology, the gelation time is defined as the time at which the elastic and viscous moduli cross. However, the gel is not fully formed at that point. In the 2.5 mg/ml collagen sample, the elastic modulus does not reach its final value until more than 45 min after the start of heating. This result is confirmed by CRM of gelation of isotropic 2.5 mg/ml collagen in the same sample cells used in the aligned collagen gel preparations. Here, the initial fibers are seen approximately 5 min after heating begins, and the visualized fibers become fixed in position at approximately 13 min after the start of heating (Fig. 4b). However, new fibers continue to form until at least 40 min after heating begins. There are differences between rheology and microscopy measurements of the kinetics of gelation (thickness of sample, perturbation during experiment, and potential slight temperature differences) that may cause the rates of gelation to differ slightly between the rheology and microscopy experiments. However, it appears that the gelation time as measured by rheology at the frequencies employed here, which correspond to shear wavelengths of several hundred microns [42], represents a similar physical event as that which occurs when the fibers become fixed in place as visualized by CRM.

While rheology measurements of 2.5 mg/ml collagen in the presence of magnetic beads have not been performed, the initial formation of fibers, the time at which they become fixed, and the time at which the final fibers are visualized are all similar to those in the plain collagen sample (Figs. 4b–e). This suggests the dynamics of gelation are not significantly different in the presence and absence of beads, though some differences were noted by Newman et al. [43]. Static images from *in situ* aligned fibrillogenesis are shown in Figs. 4d and e, and a movie of another *in situ* aligned fibrillogenesis is shown in Supplementary Movie 1 [38]. Imaging during aligned fibrillogenesis using streptavidin-coated magnetic beads shows the beads initially moving rapidly towards the poles of the external magnet

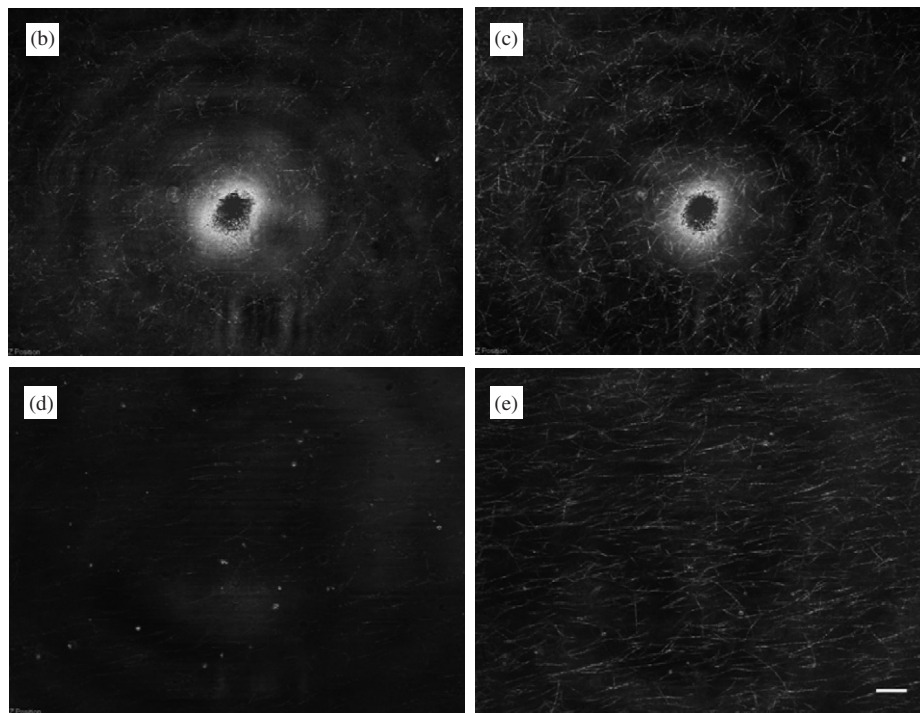
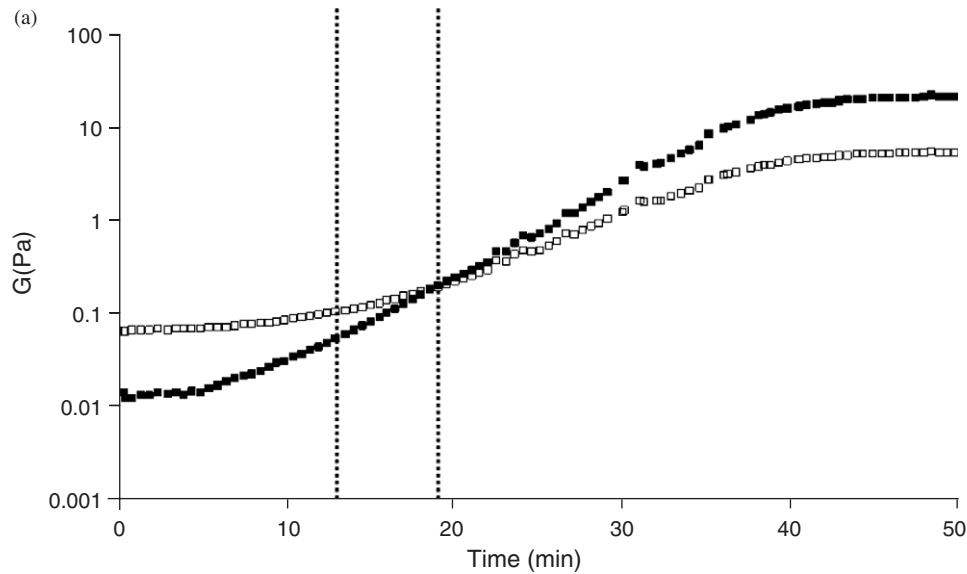


Fig. 4. (a) Elastic (■) and viscous (□) moduli of 2.5 mg/ml collagen during gelation at 1 Hz. Snapshot from movie of in situ fibrillogenesis of plain 2.5 mg/ml collagen at (b) 13 min and (c) 19 min. Snapshot from movie of in situ fibrillogenesis of collagen in the presence of streptavidin-coated magnetic beads and an external magnet at (d) 13 min and (e) 19 min. Scale bar is 15 μm and is the same in all images. The contrast is not the same in Figs. 4b and c and Figs. 4d and e, thus the brightness of speckle and fibers differ somewhat between these sets of images.

at speeds of $>100 \mu\text{m/s}$. Within 5 min, a subset of aggregates and single beads cease motion. Between 4 and 7 min after the beginning of the experiment, the first fibers are apparent. The earliest fibers tend to emerge near fixed bead clusters, and these clusters may serve as a nucleation point for fibril bundling and fiber formation. The visualized fibers lengthen only in the direction of the flow, which is apparent since some individual magnetic beads continue to move towards the magnet. By 8 min into the

experiment all bead motion ceases and (aligned) fibers are increasingly obvious. The fibers continue to appear for at least 20 min, the longest time for which in situ aligned fibrillogenesis movies were collected.

While some of the magnetic beads that become immobile early in the experiment are affixed to one of the surfaces of the sample cell, some are not. Instead, these are presumably trapped in small pores in the collagen system consisting of a network of fibrils and fibers too small to be visualized by

CRM. As mentioned, the first step in the process of gelation is self-assembly of the collagen molecules into fibrils. During this process, the viscosity and elastic modulus of the system is increasing [12,43] (Fig. 4a), though no structure is yet apparent in CRM images. The fibril formation is followed by fibril bundling into fibers. These bundles have diameters ranging from tens to hundreds of nanometers, and only those at the large end of that distribution can be visualized with CRM. In fact, even after gelation is complete it is suspected that at high-collagen concentration some of the collagen present exists in structures that are not visualized by CRM [13]. Thus, it is likely that there are small collagen structures trapping the magnetic beads even before fibers are visible in CRM. This is supported by control experiments on a sample consisting of streptavidin-coated beads, an external magnet, and water. Here, while large bead aggregates do stick to the coverslip, small clusters and single beads do not become affixed to the coverslip and continue to move within the field of view for more than 30 min.

As summarized in Table 1, magnetic beads with different surface modification lead to different degrees of alignment, with excellent alignment regularly attained with streptavidin-coated beads and very little alignment attained with unmodified beads. We believe this is because surface-modified beads are more likely to become enmeshed in collagen fibrils, and these surface-modified beads act in two ways to effect alignment. First, while moving they pull fibrils and small fibril bundles in the direction of flow, which is along the magnetic field lines. This motion aligns these small collagen structures with the flow. Because the collagen gel is likely sample-spanning before most fibers can be visualized (as evidenced by the gelation time as measured by rheology and the fact that CRM shows that early visualized fibers become immobile well before most fibers are visible), the motion of a single bead can affect the structure of fibers over relatively long distances. Second, when beads are either immobilized on the coverslip or enmeshed in collagen structures, they act as nucleating points for thick fiber bundles.

It is not surprising that streptavidin-coated beads will affix to areas dense with collagen. Streptavidin contains an Arg–Tyr–Asp (RYD) amino acid sequence that mimics the Arg–Gly–Asp (RGD) receptor domain of fibronectin [44]. Fibronectin binds to collagen I molecules, and its presence may speed up fibrillogenesis [45]. Thus, it is expected that streptavidin may also attach covalently to collagen molecules and fibrils and speed up fibrillogenesis locally. Both amine and carboxyl modified beads of at least two different sizes and preparations also give rise to aligned collagen gels, though these are neither as well aligned nor as reproducible as are those produced with streptavidin-coated magnetic beads. It has been shown previously that the onset of gelation occurs later in gelling collagen samples with large (6 μm) PS beads than without such beads [43]. However, the overall rise in viscosity is somewhat faster in bead-containing gels [43]. It was

suggested that this acceleration occurs because PS has moieties that mimic the glycosaminoglycan heparin, which is known to increase the stability of collagen fibrils [46]. In the work presented here, however, the presence of PS on the 2.5 μm magnetic beads does not appear to be an important factor in achieving aligned collagen gels. Indeed, the 1.5 μm amine and carboxyl modified beads lead to similar alignment as the 2.5 μm beads, even though the former contain no PS. Further, the unmodified beads are also coated with PS, and these do not give rise to aligned collagen. It is possible that the hydrophobicity of the unmodified PS beads leads to unfavorable energetic interactions with the collagen fibrils and fibers. This may prevent these unmodified PS beads from becoming enmeshed and entrained in the nascent collagen network on the appropriate timescale to give rise to an aligned matrix with the technique described here.

3.4. Thick gels and embedded cells

The technique to prepare thin gels described here can be extended to thicker (several millimeter) gels with relative ease. Fig. 5a presents a low-magnification CRM image of a thick 2.5 mg/ml collagen gel. Fig. 5b presents a high-magnification CRM image of a thick 1.2 mg/ml collagen, cell-bearing aligned collagen gel. As discussed in Section 2.3, the thick gels are formed in a somewhat different manner than the thin gels. However, the results are similar, with streptavidin-coated beads giving the best alignment and unmodified beads giving rise to very little alignment. C6 glioma cells have been successfully cultured in these aligned matrices. Cells are added at the same time as magnetic beads and collagen solution, and alignment is done in the presence of the cells. We find that cell survival in collagen matrices with and without streptavidin-coated magnetic beads at a concentration up to 0.2 mg/ml is similar. Thus, we do not believe streptavidin-coated iron oxide beads at these concentrations are cytotoxic, as is supported by other work [47]. The cells in the thick, cell-bearing collagen gels take several hours to spread on the collagen fibers within these gels, as they do in isotropic thick gels [13]. Once the cells spread, they align with the collagen fibers as has been seen previously in aligned collagen gels [18,21,22] (Figs. 5c and d). The glioma cells promptly begin to remodel the matrix by bundling the aligned fibers. Indeed, while there are cell-to-cell and matrix-to-matrix variations, Fig. 5 shows a typical result. Here, shortly after alignment, no cell spreading or remodeling has occurred. Several hours after alignment, however, especially in the presence of multiple cells, overall alignment is decreased as cells remodel the matrix and bundle the fibers. Future work will include optimization of formation of thick aligned collagen gels, with alignment quantified in similar ways to that presented in this manuscript for thin gels. Subsequently, we will quantify the degree of matrix remodeling that glioma cells perform in isotropic and aligned gels.

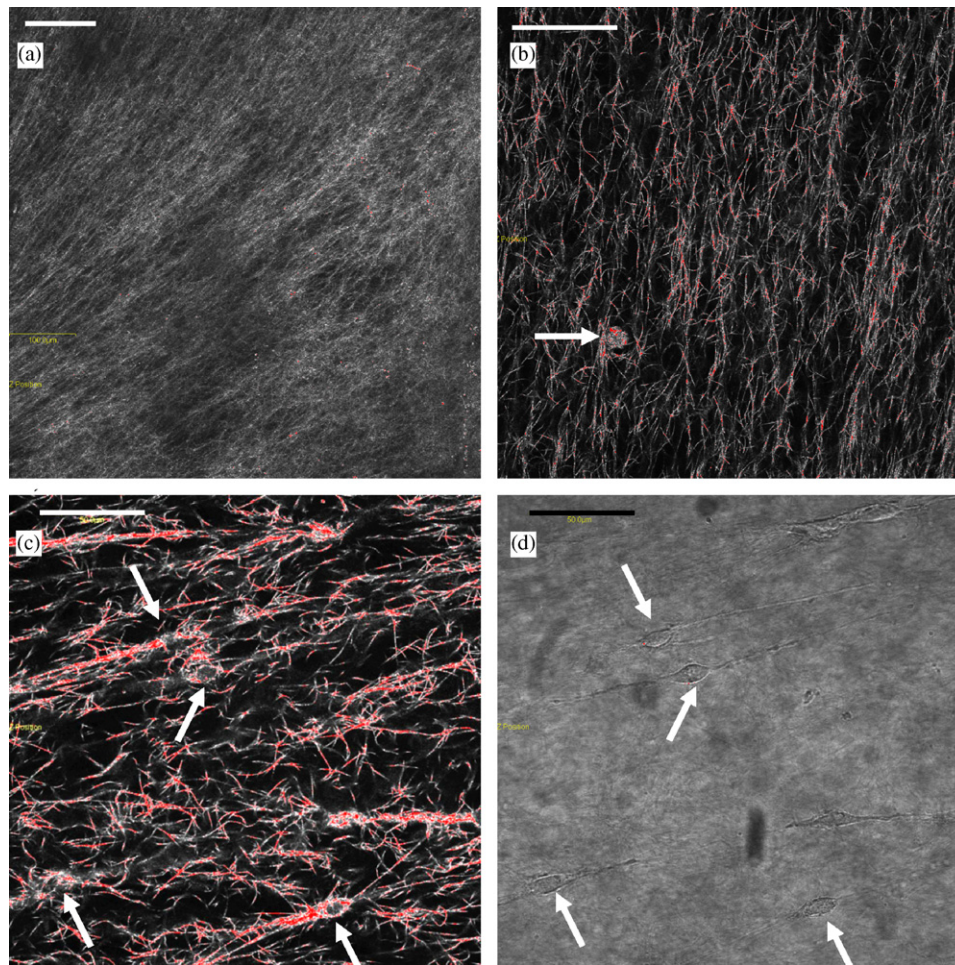


Fig. 5. (a) Low-magnification CRM image of a thick, aligned 2.5 mg/ml collagen gel without cells. (b) High magnification CRM image of a thick, aligned 1.2 mg/ml collagen, cell-bearing gel 1 h after the onset of fibrillogenesis. There is one C6 glioma cell in the field of view (arrow), which had not yet spread at the time at which the image was taken. (c) CRM image of a different thick, aligned collagen gel 10 h after the onset of fibrillogenesis. (d) DIC image of C6 glioma cells taken simultaneously with CRM image in (c). Arrows point to the nuclei of four of the cells in the field of view. Scale bar is 50 μm in all images.

4. Conclusion

We have presented a simple technique to align collagen gels. This technique achieves alignment that is qualitatively at least as good as that attained with other techniques, requires no specialized equipment, and results in aligned areas of hundreds of square microns. The alignment relies on a combination of flow and magnetic field effects. We hypothesize that beads entrained in the collagen gel *as it forms* pull fibers along the field lines produced by the external magnet. This method of alignment may be useful for building up tissue equivalents that consist of layers of aligned collagen, such as those found in bone, corneal tissue, and cartilage. The method described here also allows for the construction of gels with embedded cells. Layer by layer build up of such collagen/cell structures will be useful in forming tissue constructs. Further, embedding cells in aligned collagen gels allows for comparison of cell migration and matrix remodeling in isotropic and anisotropic surroundings that resemble the ECM present in a variety of tissues.

Acknowledgments

We thank the NYSTAR James D. Watson Program (C#040032) and Columbia University startup funds for support. We thank Yali Yang and Nina Shapely for assistance in rheology measurements and Peter Canoll for supplying C6 glioma cells.

Appendix A. Supplementary data

Supplementary data associated with this article can be found in the online version at <http://www.columbia.edu/cu/chemistry/groups/kaufman/suppmovielalignstrep060206412pmsubmit.avi>

References

- [1] Kadler KE, Holmes DF, Trotter JA, Chapman JA. Collagen fibril formation. *Biochem J* 1996;316:1–11.

- [2] Hay ED. Cell biology of extracellular matrix. New York: Plenum Press; 1991.
- [3] Ottani V, Raspanti M, Ruggeri A. Collagen structure and functional implications. *Micron* 2001;32:251–60.
- [4] Williams BR, Gelman RA, Poppke DC, Piez KA. Collagen fibril formation—optimal in vitro conditions and preliminary kinetic results. *J Biol Chem* 1978;253:6578–85.
- [5] Parkinson J, Kadler KE, Brass A. Simple physical model of collagen fibrillogenesis based on diffusion-limited aggregation. *J Mol Biol* 1995;247:823–31.
- [6] Prockop DJ, Fertala A. The collagen fibril: the almost crystalline structure. *J Struct Biol* 1998;122:111–8.
- [7] Ottani V, Martini D, Franchi M, Ruggeri A, Raspanti M. Hierarchical structures in fibrillar collagens. *Micron* 2002;33:587–96.
- [8] Leikin S, Rau DC, Parsegian VA. Temperature-favored assembly of collagen is driven by hydrophilic not hydrophobic interactions. *Nat Struct Biol* 1995;2:205–10.
- [9] Komai Y, Ushiki T. The 3-dimensional organization of collagen fibrils in the human cornea and sclera. *Invest Ophthalmol Visual Sci* 1991;32:2244–58.
- [10] Holmes DF, Gilpin CJ, Baldock C, Ziese U, Koster AJ, Kadler KE. Corneal collagen fibril structure in three dimensions: structural insights into fibril assembly, mechanical properties, and tissue organization. *Proc Natl Acad Sci USA* 2001;98:7307–12.
- [11] Brightman AO, Rajwa BP, Sturgis JE, McCallister ME, Robinson JP, Voytik-Harbin SL. Time-lapse confocal reflection microscopy of collagen fibrillogenesis and extracellular matrix assembly in vitro. *Biopolymers* 2000;54:222–34.
- [12] Forgacs G, Newman SA, Hinner B, Maier CW, Sackmann E. Assembly of collagen matrices as a phase transition revealed by structural and rheologic studies. *Biophys J* 2003;84:1272–80.
- [13] Kaufman LJ, Brangwynne CP, Kasza KE, Filippidi E, Gordon VD, Deisboeck TS, et al. Glioma expansion in collagen I matrices: analyzing collagen concentration-dependent growth and motility patterns. *Biophys J* 2005;89:635–50.
- [14] Parry DAD, Craig AS. Quantitative electron-microscope observations of collagen fibrils in rat-tail tendon. *Biopolymers* 1977;16:1015–31.
- [15] Dunn AK, Smithpeter C, Welch AJ, RichardsKortum R. Sources of contrast in confocal reflectance imaging. *Appl Opt* 1996;35:3441–6.
- [16] Strohmaier AR, Porwol T, Acker H, Spiess E. Tomography of cells by confocal laser scanning microscopy and computer-assisted three-dimensional image reconstruction: localization of cathepsin B in tumor cells penetrating collagen gels in vitro. *J Histochem Cytochem* 1997;45:975–83.
- [17] Guido S, Tranquillo RT. A methodology for the systematic and quantitative study of cell contact guidance in oriented collagen gels—correlation of fibroblast orientation and gel birefringence. *J Cell Sci* 1993;105:317–31.
- [18] Dickinson RB, Guido S, Tranquillo RT. Biased cell-migration of fibroblasts exhibiting contact guidance in oriented collagen gels. *Ann Biomed Eng* 1994;22:342–56.
- [19] Kotani H, Iwasaka M, Ueno S, Curtis A. Magnetic orientation of collagen and bone mixture. *J Appl Phys* 2000;87:6191–3.
- [20] Friedl P, Borgmann S, Brocker EB. Amoeboid leukocyte crawling through extracellular matrix: lessons from the dictyostelium paradigm of cell movement. *J Leukocyte Biol* 2001;70:491–509.
- [21] Dubey N, Letourneau PC, Tranquillo RT. Neuronal contact guidance in magnetically aligned fibrin gels: effect of variation in gel mechano-structural properties. *Biomaterials* 2001;22:1065–75.
- [22] Girton TS, Barocas VH, Tranquillo RT. Confined compression of a tissue-equivalent: collagen fibril and cell alignment in response to anisotropic strain. *J Biomech Eng-T ASME* 2002;124:568–75.
- [23] Wolf K, Muller R, Borgmann S, Brocker EB, Friedl P. Amoeboid shape change and contact guidance: T-lymphocyte crawling through fibrillar collagen is independent of matrix remodeling by MWs and other proteases. *Blood* 2003;102:3262–9.
- [24] Friedl P, Hegerfeldt Y, Tilisch M. Collective cell migration in morphogenesis and cancer. *Int J Dev Biol* 2004;48:441–9.
- [25] Friedl P. Dynamic imaging of cellular interactions with extracellular matrix. *Histochem Cell Biol* 2004;122:183–90.
- [26] Wolf K, Friedl P. Functional imaging of pericellular proteolysis in cancer cell invasion. *Biochimie* 2005;87:315–20.
- [27] Wu J, Rajwa B, Filmer DL, Hoffmann CM, Yuan B, Chiang CS, et al. Analysis of orientations of collagen fibers by novel fiber-tracking software. *Microsc Microanal* 2003;9:574–80.
- [28] Scott JE. Supramolecular organization of extracellular-matrix glycosaminoglycans, in vitro and in the tissues. *Faseb J* 1992;6:2639–45.
- [29] Benjamin HB, Pawlowski E, Becker AB. Collagen as temporary dressing and blood vessel replacement. *Arch Surg-Chicago* 1964;88:725–7.
- [30] Elsdale T, Bard J. Collagen substrata for studies on cell behavior. *J Cell Biol* 1972;54:626–8.
- [31] Mosser G, Anglo A, Helary C, Bouligand Y, Giraud-Guille MM. Dense tissue-like collagen matrices formed in cell-free conditions. *Matrix Biol* 2006;25:3–13.
- [32] Torbet J, Ronziere MC. Magnetic alignment of collagen during self-assembly. *Biochem J* 1984;219:1057–9.
- [33] Worcester DL. Structural origins of diamagnetic anisotropy in proteins. *Proc Natl Acad Sci USA* 1978;75:5475–7.
- [34] Pauling L. Diamagnetic anisotropy of the peptide group. *Proc Natl Acad Sci USA* 1979;76:2293–4.
- [35] Ng CP, Swartz MA. Fibroblast alignment under interstitial fluid flow using a novel 3-D tissue culture model. *Am J Physiol-Heart C* 2003;284:H1771–7.
- [36] Ng CP, Swartz MA. Mechanisms of interstitial flow-induced remodeling of fibroblast–collagen cultures. *Ann Biomed Eng* 2006;34:446–54.
- [37] Lee P, Lin R, Moon J, Lee LP. Microfluidic alignment of collagen fibers for in vitro cell culture. *Biomed Microdevices* 2006;8:35–41.
- [38] Guo C, Kaufman LJ. <<http://www.columbia.edu/cu/chemistry/groups/kaufman/suppmovie1alignstrep060206412pmsubmit.avi>> . 2006.
- [39] Velegol D, Lanni F. Cell traction forces on soft biomaterials. I. Microrheology of type I collagen gels. *Biophys J* 2001;81:1786–92.
- [40] George A, Veis A. FTIR in H₂O demonstrates that collagen monomers undergo a conformational transition prior to thermal self-assembly in vitro. *Biochemistry* 1991;30:2372–7.
- [41] Veis A, George A. Fundamentals of interstitial collagen self-assembly. In: Yurchenco PD, Birk DE, Mecham RP, editors. *Extracellular matrix assembly and function*. San Diego: Academic Press; 1994. p. 15–45.
- [42] Landau LD, Lifshitz EM. *Fluid mechanics*. New York: Pergamon Press; 1978.
- [43] Newman S, Cloitre M, Allain C, Forgacs G, Beysens D. Viscosity and elasticity during collagen assembly in vitro: relevance to matrix-driven translocation. *Biopolymers* 1997;41:337–47.
- [44] Alon R, Bayer EA, Wilchek M. Streptavidin contains an RYD sequence which mimics the RGD receptor domain of fibronectin. *Biochem Biophys Res Co* 1990;170:1236–41.
- [45] Speranza ML, Valentini G, Calligaro A. Influence of fibronectin on the fibrillogenesis of type-I and type-III collagen. *Collagen Relat Res* 1987;7:115–23.
- [46] Mepheron JM, Sawamura SJ, Condell RA, Rhee W, Wallace DG. The effects of heparin on the physicochemical properties of reconstituted collagen. *Collagen Relat Res* 1988;8:65–82.
- [47] Tiwari A, Punshon G, Kidane A, Hamilton G, Seifalian AM. Magnetic beads (DynabeadTM) toxicity to endothelial cells at high bead concentration: implication for tissue engineering of vascular prosthesis. *Cell Biol Toxicol* 2003;19:265–72.